A Metastable Prerequisite for the Growth of Lumazine Synthase Crystals

Olga Gliko,[†] Nikolaus Neumaier,[‡] Weichun Pan,[†] Ilka Haase,[‡] Markus Fischer,[‡] Adelbert Bacher,[‡] Sevil Weinkauf,[‡] and Peter G. Vekilov*,[†]

Contribution from the Department of Chemical Engineering, University of Houston, Houston, Texas 77204, and Department of Chemistry, Technical University Munich, Lichtenbergstrasse 4, D-85748 Garching, Germany

Received November 10, 2004; E-mail: vekilov@uh.edu

Abstract: Dense liquid phases, metastable with respect to a solid phase, form in solutions of proteins and small-molecule materials. They have been shown to serve as a prerequisite for the nucleation of crystals and other ordered solid phases. Here, using crystals of the protein lumazine synthase from *Bacillus subtilis*, which grow by the generation and spreading of layers, we demonstrate that within a range of supersaturations the only mechanism of generation of growth layers involves the association of submicrometer-size droplets of the dense liquid to the crystal surface. The dense liquid is metastable not only with respect to the crystals, but also with respect to the low-concentration solution: dynamic light scattering reveals that the droplets' lifetime is limited to several seconds, after which they decay into the low-concentration solution. The short lifetime does not allow growth to detectable dimensions so that liquid−liquid phase separation is not observed within a range of conditions broader than the one used for crystallization. If during their lifetime the droplets encounter a crystal surface, they lower their free energy not by decay, but by transformation into crystalline matter, ensuring perfect registry with the substrate. These observations illustrate two novel features of phase transformations in solutions: the existence of doubly metastable, short-lifetime dense phases and their crucial role for the growth of an ordered solid phase.

Introduction

Whether crystals grow by attachment of single atoms or molecules or by the accumulation of blocks with a proper crystalline arrangement preassembled in the nutrient medium was the topic of heated arguments in the early days of crystal growth science.[1] The preassembled block mechanisms were proven wrong by the incompatibility between the expected crystallization kinetics laws and those actually found.[1] There have been numerous observations of atomic- and molecular-scale features on surfaces of growing crystals that are only compatible with attachment of single atoms or molecules; see, for example, refs 2 and 3.

In recent years, the complexity of the substances that are crystallized, in particular from solution, has increased. Crystals of proteins are grown for the purposes of structural biology;[4] large organic molecules are crystallized in pharmaceutical processes.[5] A common feature of the solutions of such large molecules is that at ionic strengths >0.1 M, where the

characteristic Debye length of the electrostatic interactions is comparable (or, at higher ionic strengths, shorter) to the surface roughness of the protein molecules, the range of interactions between the solute molecules is largely determined by the *solvent* molecular size and is significantly shorter than the size of the *solute* molecules.[6] As a result, liquid−liquid (L−L) phase separation[7−10] in such solutions is metastable with respect to the solution-crystal equilibrium.[11−14] This metastability of the dense liquid phase with respect to the crystalline phase allows for a novel mechanism of the solution-to-crystals phase transition,[15,16] whereby dense liquid droplets serve as precursors to crystalline nuclei.[10,17,18] The possibility that the dense liquid

[†] University of Houston.

[‡] Technical University Munich.

(1) Buckley, H. E. *Crystal Growth*; Wiley & Sons: New York, 1951.

(2) McPherson, A.; Malkin, A. J.; Kuznetsov Yu, G. *Annu. Rev. Biophys. Biomol. Struct.* **2000**, *29*, 361−410.

(3) Vekilov, P. G.; Chernov, A. A. In *Solid State Physics*; Ehrenreich, H., Spaepen, F., Eds.; Academic Press: New York, 2002; Vol. 57, pp 1−147.

(4) Carter Jr., C. W., Sweet, R. M., Eds. *Macromolecular Crystallography, Part C*; Academic Press: San Diego, CA, 2003; Vol. 368.

(5) Profir, V. M.; Rasmuson, A. C. *Cryst. Growth Des.* **2004**, *4*, 315−323.

(6) Chernov, A. A.; Komatsu, H. In *Science and Technology of Crystal Growth*; van der Eerden, J. P., Bruinsma, O. S. L., Eds.; Kluwer Academic: Dordrecht, The Netherlands, 1995; pp 329−353.

(7) Broide, M. L.; Berland, C. R.; Pande, J.; Ogun, O. O.; Benedek, G. B. *Proc. Natl. Acad. Sci. U.S.A.* **1991**, *88*, 5660−5664.

(8) Casselyn, M.; Perez, J.; Tardieu, A.; Vachette, P.; Witz, J.; Delacroix, H. *Acta Crystallogr., Sect. D* **2001**, *57*, 1799−1812.

(9) Velev, O. D.; Kaler, E. W.; Lenhoff, A. M. *Biophys. J.* **1998**, *75*, 2682−2697.

(10) Galkin, O.; Chen, K.; Nagel, R. L.; Hirsch, R. E.; Vekilov, P. G. *Proc. Natl. Acad. Sci. U.S.A.* **2002**, *99*, 8479−8483.

(11) Thomson, J. A.; Schurtenberger, P.; Thurston, G. M.; Benedek, G. B. *Proc. Natl. Acad. Sci. U.S.A.* **1987**, *84*, 7079−7083.

(12) Bonnett, P. E.; Carpenter, K. J.; Dawson, S.; Davey, R. J. *Chem. Commun.* **2003**, 698−699.

(13) Wu, J.; Bratko, D.; Prausnitz, J. M. *Proc. Natl. Acad. Sci. U.S.A.* **1998**, *95*, 15169−15172.

(14) Fu, D.; Li, Y.; Wu, J. *Phys. Rev. E* **2003**, *68*, 011403.

(15) ten Wolde, P. R.; Frenkel, D. *Science* **1997**, *277*, 1975−1978.

(16) Talanquer, V.; Oxtoby, D. W. *J. Chem. Phys.* **1998**, *109*, 223−227.

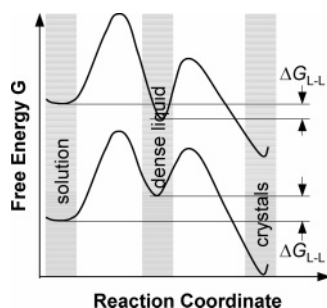**Figure 1.** Free energy G along two possible pathways from solution to crystal. The intermediate minimum is for droplets of dense liquid formed as a result of a density fluctuation, and the final minimum for crystals corresponds to structuring of the dense liquid into crystals. ΔG_{L-L} is the free energy of formation of the dense liquid phase. For the upper curve, $\Delta G_{L-L} < 0$, and the dense phase is stable with respect to the initial solution, but metastable with respect to the crystals; that is, the system is below the L−L coexistence line. For the lower curve, the system is above the L−L coexistence line, $\Delta G_{L-L} > 0$, and the dense phase is metastable with respect to both the solution and the crystals and only exists for a limited lifetime.

could also be involved in the second stage of crystal formation, that of growth of the nucleated crystals, was invoked in ref 19 as the most likely explanation of the observed growth phenomena.

In the region of the phase diagram above the L−L separation line and below the liquidus, a dense liquid droplet, arising as a result of a fluctuation, would be unstable or metastable with respect to the solution supersaturated with respect to the crystals (Figure 1). The participation of dense liquid metastable with respect not only to the new phase, the crystals, but also to the "old" solution phase in crystal nucleation or growth has never been discussed by theory or examined by experiments.

Here, we use as a test system the crystallization of the protein lumazine synthase, an icosahedral hollow capsid of 60 identical subunits[20,21] involved in the riboflavin biosynthetic pathway of *Bacillus subtilis*.[22,23] We show that dense liquid droplets can be a necessary prerequisite for the growth of crystals. We show that, in solutions of this protein, the dense liquid is metastable not only with respect to the crystals, but also with respect to the initial protein solution. Since the kinetics of decay of the dense liquid droplets into the solution are significantly faster that those of their crystallization, their lifetimes are short and do not allow their growth to macroscopic dimensions. We also show that, in a range of supersaturations, the association of dense liquid droplets to the surface of a crystal is the *only* mechanism of generation of new crystalline layers. Thus, the preassembly of dense droplets is an essential prerequisite for crystallization, although these droplets are substantially different from the preordered blocks envisioned in the early days of crystallization science.[1] In further deviation from the early preassembly
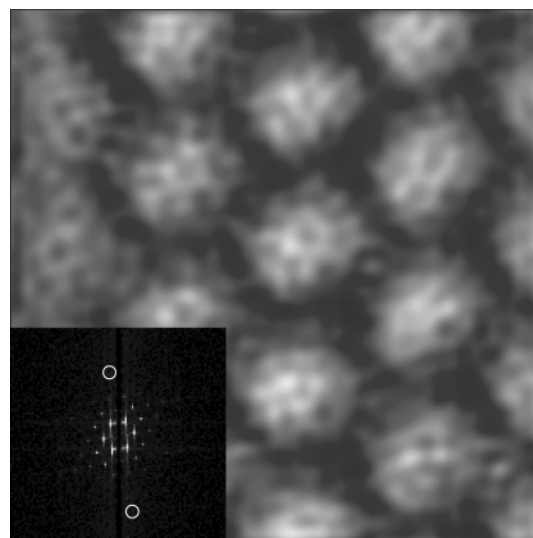
(17) Galkin, O.; Vekilov, P. G. *Proc. Natl. Acad. Sci. U.S.A.* **2000**, *97*, 6277−6281.
(18) Vekilov, P. G.; Galkin, O. In *Nanoscale Structure and Assembly at Solid-fluid Interfaces. Vol. II: Assembly in Hybrid and Biological Systems*; DeYoreo, J. J., Lui, X. Y., Eds.; Kluwer Academic: New York, 2004; pp 105−144.
(19) Kuznetsov, Y. G.; Malkin, A. J.; McPherson, A. *Phys. Rev. B* **1998**, *58*, 6097−6103.
(20) Schott, K.; Ladenstein, R.; König, A.; Bacher, A. *J. Biol. Chem.* **1990**, *265*, 12686−12689.
(21) Ritsert, K.; Huber, R.; Turk, D.; Ladenstein, R.; Schmidt-Bäse, K.; Bacher, A. *J. Mol. Biol.* **1995**, *253*, 151−167.
(22) Bacher, A.; Eberhardt, S.; Fischer, M.; Kis, K.; Richter, G. *Annu. Rev. Nutr.* **2000**, *20*, 153−167.
(23) Bacher, A.; Baur, R.; Eggers, U.; Harders, H.; Otto, M. K.; Schnepple, H. *J. Biol. Chem.* **1980**, *255*, 632−637.

Figure 2. Image of a 100×100 nm^2 area from a (001) face of a lumazine synthase crystal. Pentagonal and trigonal arrangements of submolecular features are well detectable.[53,56] Inset: Fourier transform of image illustrates hexagonal symmetry of molecular arrangement in the (001) face; sixth-order peaks, corresponding to resolution of 1.6 nm have been circled. The anisotropy of the spot pattern is due to inherently anisotropic image acquisition, with significant differences between the slow (x) and fast (y) scanning directions.

scenarios, the droplets are only required for the generation of new layers, which then grow by the incorporation of single molecules.

Methods

Solubility and Crystallization Kinetics of Lumazine Synthase. Lumazine synthase of *B. subtilis* was expressed in a recombinant *B. subtilis* strain and purified according to published procedures.[24] The molecular mass is $\sim 10^6$ g mol^{-1}, and its diameter is ~ 15.6 nm.[20] The protein solutions used contained from 1 to 30 mg mL^{-1} of lumazine synthase in 0.1−1.5 M sodium/potassium phosphate at pH = 8.7 and 1 mM 5-nitro-6-ribitylamino-2,4($1H,3H$)-pyrimidinedione, an enzyme inhibitor that enhances the stability of the molecule. These solutions were filtered through a 0.22 μm syringe filter.

Crystals grown from these solutions are hexagonal, with space group $P6_322$, and facetted by basal {001} and prismatic {100} faces.[24] The growth of the {001} faces was monitored in situ using an atomic force microscope (AFM, Nanoscope IIIa, from Veeco, Inc., Santa Barbara, CA) in the tapping mode. The crystals were nucleated in 10 μL droplets of 10 mg mL^{-1} solutions in 1.3−1.5 M phosphate on electron microscopy grids cemented to Teflon-coated metal disks. These were then transferred to the fluid cell of the AFM, and the cell was filled with solution of the chosen protein and buffer concentrations. The scanning parameters were adjusted so that continuous imaging affected neither the crystal surface nor the process dynamics (for details, see ref 25). The resolution up to 1.6 nm of our imaging allowed ready distinction of individual molecules and some submolecular details; see Figure 2.

The basal faces of lumazine synthase crystals grow by generation and spreading of layers, as seen before.[24] To determine the solubility of lumazine synthase at the chosen temperature of 24 °C, we monitored the propagation of growth steps, the edges of the unfinished layers on the crystal surface, at different solution concentrations. In Figure 3, AFM images with disabled slow axes show slow forward step

(24) Braun, N.; Tack, J.; Fischer, M.; Bacher, A.; Bachmann, L.; Weinkauf, S. *J. Cryst. Growth* **2000**, *212*, 270−282.
(25) Yau, S.-T.; Petsev, D. N.; Thomas, B. R.; Vekilov, P. G. *J. Mol. Biol.* **2000**, *303*, 667−678.
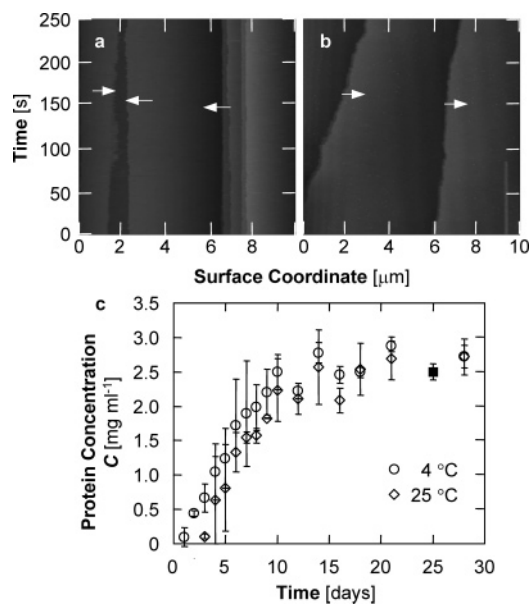
Figure 3. Solubility of lumazine synthase crystals in 1.3 M phosphate buffer with pH = 8.7. (a) and (b) Growth steps at different protein concentration at 24 °C. AFM images with disabled slow axes. Brighter color indicates greater value of *z*-axis, perpendicular to image. Arrows indicate directions of step motion. (a) Slow forward step movement at $C = 2.5$ mg mL^{-1}. (b) Fast retreating steps at 2.3 mg mL^{-1}. (c) The evolution of the protein concentration in an undersaturated solution in contact with dissolving crystals at 4 and 25 °C. The saturation value was taken as solubility, and the value of C_e at both temperatures agrees well with the value of 2.5 mg mL^{-1} from (a) and (b) for 24 °C, indicated as ■.

movement at $C = 2.5$ mg mL^{-1} and faster backward movements at $C = 2.3$ mg mL^{-1}. Thus, we chose as a solubility value $C_e = 2.5 \pm 0.1$ mg mL^{-1}.

For an independent test of the solubility value and in search of temperature dependence of the solubility, we monitored by the Bradford assay[26] the concentration of undersaturated solutions held at 4 and 25 °C as we continuously added crystals from another batch to the container. The time evolution curves of the protein concentration at two temperatures, 4 and 25 °C, are shown in Figure 3c. The steady concentration values, achieved after ~20 days, were taken as solubilities. Figure 3c shows that the solubility does not depend on temperature, and the value stemming from the batch runs agrees well with the one from the AFM determination.

The step velocities were measured by disabling the slow scanning axis of the AFM.[27] The data, showing the location of the step as a function of the time of observation, are similar to those in Figure 3a and b. The velocities determined from the locations of steps in different scan lines were averaged, so that a mean step velocity is the result of averaging over 20–30 independent determinations. Supersaturation was imposed by pumping solution with $C > C_e$ into the cell, and the driving force for crystallization $\sigma \equiv \{\exp[-(\mu_c - \mu_s)/k_BT] - 1\}$ was calculated as $\sigma \approx (C/C_e - 1)$; subscripts **c** and **s** denote crystal and solute, respectively, and subscript **e** denotes equilibrium. The approximate equality is based on the expressions for the respective chemical potentials $\mu_s = \mu_0 + k_BT \ln(\gamma C)$ and $\mu_c = \mu_0 + k_BT \ln(\gamma_e C_e)$, with the activity coefficients $\gamma \approx \gamma_e \approx 1$ for solutions of concentrations <5 mg mL^{-1} = 5 μmol L^{-1}, employed in the crystallization runs.

Dynamic Light Scattering Characterization of Lumazine Synthase Solution. Dynamic light scattering data were collected at 20 °C in 8 or 10 mm cylindrical cuvettes at an angle of 60°, employing either an AXIOS-150 (Triton-Hellas) apparatus with a 35 mW diode laser operating at a wavelength of 658 nm or an ALV static and dynamic

light scattering device with a 22 mW He−Ne laser with a wavelength of 632.8 nm. Spectra were recorded every 30 s for at least 2 h. The particle distributions were obtained using Provencher's regularized Laplace-inversion CONTIN algorithm for the autocorrelation function.[28,29] The scatterers form factors were approximated by those of spheres. The characteristic sizes stemming for select autocorrelation functions were verified by exponential fits to the data.[30]

Results and Discussion

The Mechanisms of Layer Generation and Step Propagation. We monitored the growth of {001} faces of lumazine synthase crystals on which the molecules have hexagonal coordination. At driving forces $\sigma > 2$, the growth layers are generated by 2D nucleation, with numerous circular islands seen on the surface of the crystals. This mode of layer generation has been found for crystals of many other proteins[31−35] and is known to require a driving force above a threshold.[36] No 2D nucleation was observed at $\sigma < 2$. Furthermore, no dislocations, an alternative source of layers, operational even at low supersaturations,[31,37] were seen outcropping on faces of lumazine synthase crystals, likely because of the large elastic energies associated even with the minimal Burgers vector allowed by the crystal structure: 15.6 nm. (The elastic stress of a dislocation scales with the square of the Burgers vector and is proportional to the Young modulus.[38] The Young modulus is known for only one protein crystal, lysozyme, and is comparable to that of small-molecule crystals.[3,39]) However, the crystals grow even at driving forces as low as $\sigma \approx 0.5$. Searching for the source of growth layers, we consistently saw that the new layers originate from events similar to the one represented by the sequence in Figure 4.

As in Figure 4a, clusters landed on the crystal surface between existing steps. While the lateral dimensions of the clusters could not be judged from the image, their height was reliably determined: it varied between ~100 and 160 nm, and in Figure 4g, it was ~120 nm. The clusters then grew sideways and became integral parts of the crystal, generating, in Figure 4b−f, five new layers.

Three facts stemming from Figure 4 convince us that these are droplets of dense liquid: (i) The clusters shrink in height as they rest on the crystal surface and grow laterally (compare Figure 4g and h), (ii) the layers originating from the clusters merge continuously with each other and with the underlying lattice, and (iii) the velocity of the layers originating from a cluster is the same as the velocity of the other layers on the surface of the crystal. If these were crystalline clusters, the

(26) Bradford, M. M. *Anal. Biochem.* **1976**, *15*, 248−254.
(27) Kitamura, N.; Lagally, M. G.; Webb, M. B. *Phys. Rev. Lett.* **1993**, *71*, 2081−2085.
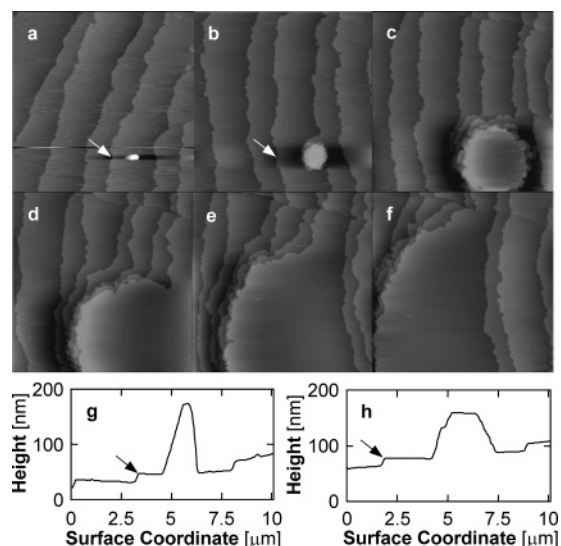(28) Provencher, S. W. *Comput. Phys. Commun.* **1982**, *27*, 213−227.
(29) Provencher, S. W. *Comput. Phys. Commun.* **1982**, *27*, 229−242.
(30) Schmitz, K. S. *Dynamic Light Scattering by Macromolecules*; Academic Press: New York, 1990.
(31) Vekilov, P. G.; Rosenberger, F. *J. Cryst. Growth* **1996**, *158*, 540−551.
(32) McPherson, A.; Malkin, A. J.; Kuznetsov, Y. G. *Annu. Rev. Biomol. Struct.* **2000**, *20*, 361−410.
(33) McPherson, A.; Malkin, A. J.; Kuznetsov, Y. G.; Plomp, M. *Acta Crystallogr., Sect. D* **2001**, *57*, 1053−1060.
(34) Lin, H.; Yau, S.-T.; Vekilov, P. G. *Phys. Rev. E* **2003**, *67*, 0031606.
(35) Vekilov, P. G.; Feeling-Taylor, A.; Hirsch, R. E. In *Hemoglobin Disorders: Molecular Methods and Protocols*; Nagel, R. L., Ed.; Methods in Molecular Medicine Series 82; Humana Press: Totawa, NJ, 2003.
(36) Chernov, A. A.; Rashkovich, L. N.; Smol'sky, I. L.; Kuznetsov, Y. G.; Mkrtchan, A. A.; Malkin, A. I. In *Growth of Crystals*; Givargizov, E. E., Ed.; Consultant Bureau: New York, 1986; Vol. 15.
(37) Burton, W. K.; Cabrera, N.; Frank, F. C. *Philos. Trans. R. Soc. London, Ser. A* **1951**, *243*, 299−360.
(38) Van den Hoek, B.; Van der Eerden, J. P.; Bennema, P. *J. Cryst. Growth* **1982**, *56*, 621−632.
(39) Chernov, A. A. *J. Struct. Biol.* **2003**, *142*, 3−21.

Figure 4. Sedimentation of a 3D object in (a) and its development into a stack five crystalline layers in (b)−(f) in a lumazine synthase solution of 3 mg mL^{-1} in 1.3 M phosphate buffer at pH = 8.7. Tapping mode AFM imaging with scan size is 20 × 20 μm, and time interval between images is 9 min. (g) and (h) Height profiles along a horizontal line crossing a 3D object in (a) and (b), respectively, show the object height of ∼120 nm immediately after sedimentation in (a) and ∼75 nm in (b). Arrows in (a), (b), (g), and (h) mark the same step.
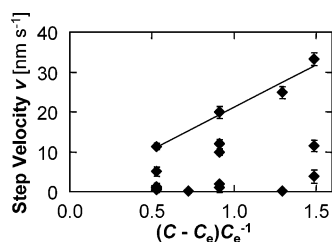

Figure 5. Quantification of the step kinetics on the (001) face of lumazine synthase crystals. The step kinetic coefficient $\beta = 4.3 \times 10^{-4}$ cm s^{-1} is estimated from a linear regression fit to the maximum values of v. For discussion, see text.

probability of them landing with a {001} plane downward and rotating to a perfect registry with the underlying lattice would be negligible. Numerous examples of microcrystals landing on surfaces of growing crystals out of registry and getting incorporated with major stacking defects have been reported.[40,41] Disordered solid clusters would not shrink in size, and the generation of new layers would likely be accompanied by the creation of a strained shell that would delay the spreading of the layers started by the clusters.

Figure 5 quantifies the kinetics of growth of steps on a (001) face of lumazine synthase crystals. For any given concentration, the average step velocity v changes significantly from one determination to another. Assuming that transport of material from the solution to the crystal surface plays a significant role in the control of the growth of the lumazine synthase crystals (for support see below), we conclude that the step velocity variations likely reflect the variations in interfacial supersaturation as a result of stirring by the AFM tip and cantilever and other random factors. Since the variation in surface concentration can never bring it above its value in the solution bulk, we assume

that maximal v-values recorded are closer to the bulk solution concentration and use them to determine the value of the step kinetic coefficient β. This β is defined as the coefficient of proportionality between the crystallization driving force σ and the step velocity $v = \beta\Omega C_e\sigma$, where the dimensionless product ΩC_e, with Ω being the molecular volume in the crystal and C_e recalculated in molecules per unit volume, accounts for the change in number density of the molecules between the solution and the crystal. Because of the above inaccuracies of the determination of the interfacial σ, the data in Figure 5 only yield a rough estimate for $\beta = 4.3 \times 10^{-4}$ cm s^{-1} from a linear regression fit to the maximum values in Figure 5.

To decide between transport and surface kinetics controlled crystal growth, we compare the face kinetic coefficient, the product βp, where p is the slope of the vicinal surface, created by the train of steps, to the characteristic rate of diffusive transport through the solution D/δ.[42] The ratio of these two expressions was introduced as a kinetic Peclet number $Pe_k = \beta p\delta/D$.[42,43] We use $p = 2 \times 10^{-2}$ from, for example, Figure 4, and diffusivity of lumazine synthase molecules $D = 1.5 \times 10^{-7}$ cm^2 s^{-1}, determined by dynamic light scattering; see below. We assume that the diffusion layer thickness δ is largely determined by buoyancy-driven convection and should be comparable to the average size of the crystals used in these determinations,[44−46] that is, $\delta \approx 3 \times 10^{-2}$ cm. Thus, we get $Pe_k = 1.7$. Note that lower values of p that are sometimes recorded would yield lower values of Pe_k. Since values of $Pe_k \approx 1$ are taken as indication of mixed transport and kinetics control of the growth process, we conclude that this is the case for the studied protein.[42]

Lack of Long-Lifetime Dense Liquid Phase in Solutions of Lumazine Synthase. Searching for independent evidence for the existence of a dense liquid phase in solutions of lumazine synthase, we investigated the phase behavior of solutions under a range of conditions broader than those where crystallization was studied by AFM. We kept solution samples with protein concentration in the range 3−30 mg mL^{-1} and buffer concentration in the range 1.3−1.5 M at temperatures ranging from 40°C (determined by the protein stability to denaturation) to −4 °C (below which the solution freezes) and monitored them with differential interference contrast optics, sensitive to any phase heterogeneity larger than 0.5 μm. We found no evidence of formation of dense liquid droplets larger than the detection size.

A possible explanation for the lack of macroscopic dense liquid phase starts with understanding why metastable dense liquid phases in solutions of other proteins are observable. The dense liquids seen with the proteins lysozyme, γ-crystalline, hemoglobin A, C, and S, with large organic molecules[7,10,12,47−49] and others are metastable with respect to an ordered solid phase

(40) Malkin, A. J.; Kuznetsov, Y. G.; McPherson, A. *J. Struct. Biol.* **1996**, *117*, 124−137.
(41) Yau, S.-T.; Thomas, B. R.; Galkin, O.; Gliko, O.; Vekilov, P. G. *Proteins: Struct., Funct., Genet.* **2001**, *43*, 343−352.
(42) Vekilov, P. G.; Thomas, B. R.; Rosenberger, F. *J. Phys. Chem. B* **1998**, *102*, 5208−5216.
(43) Vekilov, P. G.; Alexander, J. I. D. *Chem. Rev.* **2000**, *100*, 2061−2089.
(44) Lin, H.; Rosenberger, F.; Alexander, J. I. D.; Nadarajah, A. *J. Cryst. Growth* **1995**, *151*, 153−162.
(45) Lin, H.; Petsev, D. N.; Yau, S.-T.; Thomas, B. R.; Vekilov, P. G. *Cryst. Growth Des.* **2001**, *1*, 73−79.
(46) Vekilov, P. G.; Alexander, J. I. D.; Rosenberger, F. *Phys. Rev. E* **1996**, *54*, 6650−6660.
(47) Muschol, M.; Rosenberger, F. *J. Chem. Phys.* **1997**, *107*, 1953−1962.
(48) Petsev, D. N.; Wu, X.; Galkin, O.; Vekilov, P. G. *J. Phys. Chem. B* **2003**, *107*, 3921−3926.
(49) Chen, Q.; Vekilov, P. G.; Nagel, R. L.; Hirsch, R. E. *Biophys. J.* **2004**, *86*, 1702−1712.

of the respective proteins but, very importantly, are stable; that is, they have lower free energy than the initial low-density solution. After small droplets of such dense liquids form, their lifetime is limited by two events: decay into the initial solution or transformation into an ordered solid phase. The former is thermodynamically unfavorable; the latter is extremely slow.[50] As a result, in these other systems the lifetime of the droplets is sufficient to allow growth to detectable dimensions of several or even several ten or hundred micrometers.[51]

The lack of macroscopic dense liquid phases in solutions of lumazine synthase indicates that the region in which such phases are stable with respect to the initial solution is outside of the tested area in the (temperature, concentration) plane. We would like to tentatively correlate this possibility with the independence of the solubility of the crystals on temperature: recent Monte Carlo simulations have shown that if the intermolecular interaction potential possesses a maximum at intermolecular separations longer than those of the main attractive minimum, the solubility of the crystals does not depend on temperature and the metastable L−L separation is pushed to low temperatures (S. Brandon et al., unpublished data). Those simulations document a lowering of the temperature of the L−L separation due to repulsive maxima occupying the range 0.5−0.7 molecular diameters from the molecular surface, with stronger effects if the repulsive maximum is closer to the molecular surfaces. A potential with a repulsive maximum is a natural assumption for lumazine synthase; such potentials are an adequate representation of the water-structuring (hydration and hydrophobic) interactions.[52] In the hexagonal lumazine synthase crystals, the intermolecular contacts occur along the icosahedral 3-fold and 2-fold axes;[53] while the locations where the 3-fold axes pierce the molecule's surface contain an abundance of charged and hydrophilic amino acid residues, the respective sites of the 2-fold axes are hydrophobic.[21] For water-structuring interactions, one would expect a repulsive maximum starting at one or two water molecular sizes from the surface of the protein molecule and reaching up to several water molecular sizes;[52] that is, within the range of Monte Carlo predictions of strong lowering of the L−L separation temperatures.

Short-Lifetime Dense Liquid Droplets. Probing for dense liquid droplets of sizes below the resolution limit of optical microscopy and/or short lifetimes, we carried out dynamic light scattering characterization of lumazine synthase solutions with buffer concentrations in the range 0.1−1.5 M and protein concentrations in the range 1.1−9.5 mg mL^{-1}. Data collection was initiated immediately after solution mixing and was repeated every 30 s for ∼2−4 h. In all such runs with buffer concentration below 1.5 M, more than 80 or 90% of all collected autocorrelation functions were similar to the one shown as the lower curve in Figure 6a. The good fit to an exponentially decaying function of the delay time τ reveals the presence of a single scatterer with diffusivity $D = 1.5 \times 10^{-7}$ cm^2 s^{-1}.[30] According to the Stokes law, the size of these scatterers is ∼16.5 nm, consistent with the radius of hydrated lumazine synthase molecules.
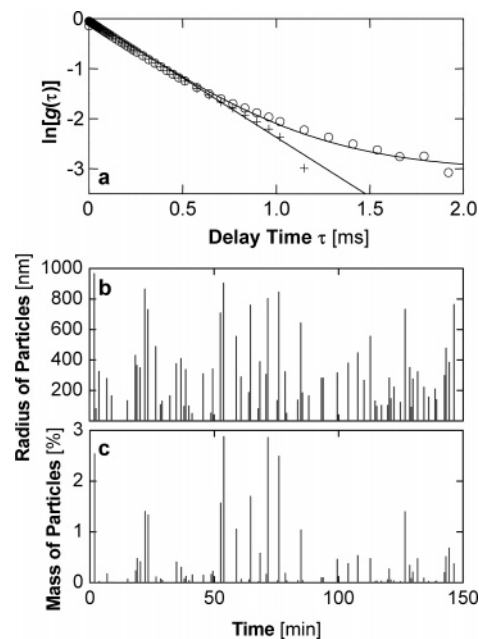
(50) Galkin, O.; Vekilov, P. G. *J. Mol. Biol.* **2004**, *336*, 43−59.
(51) Shah, M.; Galkin, O.; Vekilov, P. G. *J. Chem. Phys.* **2004**, *121*, 7505−7512.
(52) Leckband, D.; Israelachvili, J. *Q. Rev. Biophys.* **2001**, *34*, 105−267.
(53) Bacher, A.; Weinkauf, S.; Bachmann, L.; Ritsert, K.; Baumeister, W.; Huber, R.; Ladenstein, R. *J. Mol. Biol.* **1992**, *225*, 1065−1073.

Figure 6. Dynamic light scattering characterization of supersaturated solutions of lumazine synthase with $C = 8.1$ mg mL^{-1} in 1.3 M phosphate buffer with pH = 8.7. Autocorrelation functions were collected every 30 s over 3 h. (a) Representative field autocorrelation functions $g(\tau)$: + illustrates ∼90% of all cases, in which the autocorrelation function is fitted by a single-exponential decay function of the delay time τ; ○ illustrates ∼10% of the cases in which the autocorrelation function is fitted by the sum of two decaying exponents. The slope of the line through the data points decreases from a value corresponding to lumazine molecules to that of a population of scatterers with radius of ∼220 nm. (b) Time evolution of average sizes of aggregates populations. (c) Time evolution of approximate mass fraction of the protein contained in the aggregates. Data points in (b) and (c) were determined from data similar to ○ in (a). Data sets yielding autocorrelation functions similar to + in (a), that is, $R = 8$ nm, mass fraction = 100%, are not represented in (b) and (c).

However, even among the first collected autocorrelation functions we found those that deviate from the exponential decay with τ (Figure 6a). Most of these autocorrelation functions, whose total weight is ∼10−20% of all records, are well fit by the sum of two exponential decay members. The increment of the first exponent corresponds, as above, to the diffusivity and size of single lumazine synthase molecules, while the slower increment of the second exponent reveals the presence of a population of scatterers with a characteristic radius that varies between several ten and several hundred nanometers. The radii of the two scatterers and the mass fraction of the large species were evaluated by the CONTIN procedures and are plotted in Figure 6b and c as functions of the time after the beginning of light scattering data collection, in which the majority of the cases with a single population of lumazine synthase molecules are reflected as $R = 0$. In <1% of all collected data, the autocorrelation functions were best fit by sums of three exponential decays. Such fits are deemed unreliable, and these data were ignored.

In Figure 6b, the times between detection of large scatterers vary from 30 s to 6 min with a mean of ∼2 min; the mean radius of the large scatterers is $\bar{R} \approx 280$ nm. The time correlation function $\langle [R(t + \Delta t) - R(t)]^2 \rangle_{\Delta t}$ of the radii of the scatterers reaches saturation at $<R^2> \approx 8 \times 10^4$ nm^2, corresponding to the above $\bar{R}$, after $\Delta t \approx 2$ min, the mean time between detection of large scatterers, and, significantly, remains steady at longer times.

Other Possible Large Scatterers. Numerous repetitions of the experiments illustrated in Figure 6 always showed the presence of the large scatterers randomly appearing and disappearing throughout the data collection time, with approximately reproducible mean sizes and average times between detection. Tests with deionized water and low-concentration phosphate buffers showed a lack of any scattering populations, while phosphate buffers at concentrations 0.5−1.3 M revealed scatterers of sizes of a few nanometers, much smaller than the lumazine synthase and the large scatterers; these are, likely, phosphate ion oligomers.[54]

In samples of buffer concentration >1.4 M and protein concentration >3−5 mg mL^{-1}, after ∼30 min a population of scatterers is superimposed on those similar to the one in Figure 6b, and in another ∼15 min is the only one reflected in the light scattering signal. After this population appears, the autocorrelation function never goes back to a single-exponential decay, and the radii and mass fraction of these scatterers grow indefinitely. After ∼1.5 h, numerous tiny hexagonal lumazine synthase crystals are detectable in the cuvette. We conclude that this growing population of scatterers consists of crystalline nuclei and supercritical crystallites of the protein.

The lack of increasing or decreasing trends of the population of large scatterers in Figure 6b, reflected in the steady part of the time correlation function of their sizes, discussed above, convince us that the large scatterers are not permanent objects (single or populations thereof), which wander in and out of the probing beam, but rather appear and disappear uniformly throughout the whole solution volume. A detailed investigation of the ordered and disordered condensed phases in solutions of lumazine synthase in phosphate buffers has shown that at the buffer concentration of 1.3 M of our crystallization experiments, crystals and a disordered liquid or solid are the only condensed phases.[55] To test if the large clusters are crystals, we note that their estimated rates of growth and decay are >10 nm s^{-1}: significantly faster than the rates of growth and dissolution of crystals $R = pv \approx 0.2-0.7$ nm s^{-1}. In combination with the distinctive signature of the light scattering signal from nucleating and growing crystals at higher buffer concentrations, and with the similarity of the data in Figure 6 to those in solutions undersaturated with respect to crystals, these estimates mean that the large scatterers are not crystals.

On the other hand, fast nucleation and growth and decays rates have been shown for dense liquid droplets in protein solutions.[51] This and all other pieces of evidence discussed above lead us to the conclusion that the large scatterers are droplets of a dense liquid phase. The short lifetimes of these droplets indicate that they have a free energy higher than not only the crystals, but also the low-concentration solution. Their measurable lifetime suggests that a barrier, either thermodynamic or kinetic, for the droplets' decay exists; that is, they are metastable and not unstable with respect to the initial state, as schematically depicted by the lower curve in Figure 1.

The existence of metastable droplets in a solution, which is undersaturated with respect to the dense liquid phase, is not a trivial conclusion: only unstable droplets exist, for instance, in undersaturated vapors of small-molecular substances. While a fuller understanding of their thermodynamic and kinetic causes is still lacking, their presence in the solution seems well documented by the experiments discussed above and illustrated by Figure 6.

The Crystal Growth Scenario. The participation of the metastable dense liquid droplets in the growth process illustrated by Figure 4 can be understood in the following way. The metastable liquid phase droplets are characterized by short lifetimes, high molecular density (comparable to that in a solid state), and high mobility of the protein molecules. When a droplet encounters the crystal surface, it is stabilized: under the influence of the periodic field of the crystal, in which the protein molecules are oriented so that the hydrophobic patches of their surfaces are in contact, long-range order is imposed in the dense liquid droplets and they transform into stacks of crystalline layers. The spreading of these layers due to the attachment of single molecules form the solution results in crystal growth. As discussed above, the association to the crystal and structuring of metastable droplets of protein-rich liquid is the only mechanism providing for crystal growth.

Conclusions

Using a combination of dynamic light scattering, atomic force microscopy, and bulk solution determinations, we demonstrate two novel features of phase behavior of proteins and, likely, other large molecules in solution: the presence of dense liquid droplets, which are metastable not only with respect to the growing crystals, but also with respect to the low-concentration protein solution, and their crucial role for the growth of the ordered solid phase. In contrast to previous observations, the droplets do not promote the nucleation of crystals, but rather play a crucial role in crystal growth stage: the encounter of a droplet and the crystal surface, followed by structuring, results in the formation of stacks of crystalline layers. Since dislocation sources are missing at the studied surfaces and the supersaturations are insufficient for two-dimensional nucleation of new layers, the droplets of the dense liquid associating to the crystal are the only source of growth layers.

JA043218K

(54) Ceretta, M. K.; Berglund, K. A. *J. Cryst. Growth* **1987**, *84*, 577−588.
(55) Rodrigez Fernandez, L. *Crystallization of lumazine synthase from Bacillus subtilis*: electron microscopic observations. Ph.D. Thesis, Technical University of Munich, Munich, Germany, 2003.
(56) Weinkauf, S.; Bacher, A.; Baumeister, W.; Ladenstein, R.; Huber, R.; Bachmann, L. *J. Mol. Biol.* **1991**, *221*, 637−645.